

## The wave-mode purity in ECRH: advanced 3D ray-tracing modeling for W7-X

I. Vakulchyk, P. Aleynikov, N.B. Marushchenko

*Max Planck Institute for Plasma Physics, Wendelsteinstr. 1, 17491 Greifswald, Germany*

Since the power density of the narrow RF beam applied for ECRH in W7-X is quite high (up to  $\text{GW}/\text{m}^2$  within the beam-spot), the requirements on wave-mode purity are also high. In particular, any polarization mismatch at the entrance into the plasma should be minimized. In experiments, however, the wave-mode purity can be significantly reduced due to, for example, coupling with the spurious wave-mode in the sheared magnetic field, due to high inhomogeneities, scrambling on the mirror during re-entrance in multi-pass scenarios, etc. The exchange of the energy between coupled modes for the case when both the primary and spurious waves propagate in one dimension has been extensively studied (see for example [1, 2, 3] and references therein).

In W7-X, with  $B_0 \simeq 2.5$  T and ECR heating at 140 GHz, the X2-mode is used for moderate density scenarios, up to  $10^{20} \text{ m}^{-3}$ , while for higher densities a use of the O2-mode is the main scenario. An oblique injection is standard in both cases. As a consequence, at the plasma periphery where the density gradient is highest, the refraction is usually significant. Furthermore, if the spurious mode appears, an unwanted birefringence also takes place.

The aim of present work is to develop a heuristic model, suitable for an implementation in ray-tracing code TRAVIS [4], which would include both the mode coupling effects and possible splitting of the beams, as well as geometrical effects related to the curved ray trajectory.

We construct a coordinate system  $s, v, w$  linked to the reference ray trajectory  $\mathbf{R}_r$  calculated by ray-tracing for the desired wave mode in the following way:  $s$  is the arc-length along the ray, the wave vector has zero  $v$  component,  $\mathbf{k}_v = 0$ , and a tangent to the ray vector is  $\mathbf{t} = \partial \mathbf{R}_r / \partial s$

$$\mathbf{e}_s = \mathbf{t} + v\mathbf{e}'_v + w\mathbf{e}'_w, \quad \mathbf{e}_v = (\mathbf{N} \times \mathbf{t}) / |\mathbf{N} \times \mathbf{t}|, \quad \mathbf{e}_w = (\mathbf{N} - \mathbf{t}(\mathbf{N} \cdot \mathbf{t})) / |\mathbf{N} - \mathbf{t}(\mathbf{N} \cdot \mathbf{t})|. \quad (1)$$

Here,  $\mathbf{N} = \frac{c}{\omega} \mathbf{k}$  is a normalized wave vector and primes indicate derivatives along the ray,  $d/ds$ . Since the wave front is not necessarily perpendicular to the ray, the eikonal can be represented as a sum of components tangential and normal to the ray,  $\mathbf{k} \cdot \mathbf{r} = \frac{\omega}{c} (N_t s + N_n w)$ . We use this fact and rewrite Maxwell equation in  $(s, v, w)$  coordinates and take the limit  $v, w \rightarrow 0$ , which only accounts for the close vicinity of the ray and reduce the problem to a system for  $\mathbf{f} = \{E_w, E_v, B_w, B_v\}$ ,

$$\frac{d\mathbf{f}}{ds} = i \frac{\omega}{c} \hat{T} \mathbf{f}, \quad \hat{T} = \hat{T}_{\text{wave}} + \hat{R} \quad (2)$$

where  $\hat{T}$  represents the wave propagation matrix with the main part  $\hat{T}_{wave}$  describing the mode coupling:

$$\hat{T}_{wave} = \begin{pmatrix} -\frac{\epsilon_{sw}^r}{\epsilon_{ss}^r}(N_n + \Lambda_{ws}) & -\tau_\lambda - \frac{\epsilon_{sv}^r}{\epsilon_{ss}^r}(N_n + \Lambda_{ws}) & 0 & \frac{N_n(N_n + \Lambda_{ws})}{\epsilon_{ss}^r} - 1 \\ \tau_\lambda - \Lambda_{ws}\frac{\epsilon_{sw}^r}{\epsilon_{ss}^r} & -\Lambda_{vs}\frac{\epsilon_{sv}^r}{\epsilon_{ss}^r} & 1 & \Lambda_{vs}N_{per} \\ \epsilon_{vw}^r - \frac{\epsilon_{sw}^r\epsilon_{vs}^r}{\epsilon_{ss}^r} & \epsilon_{vv}^r - \frac{\epsilon_{sv}^r\epsilon_{vs}^r}{\epsilon_{ss}^r} - N_n(N_n + \Lambda_{ws}) & 0 & -\tau_\lambda + \frac{\epsilon_{vs}^r}{\epsilon_{ss}^r}N_n \\ -(\epsilon_{ww}^r - \frac{\epsilon_{sw}^r\epsilon_{ws}^r}{\epsilon_{ss}^r}) & -(\epsilon_{vv}^r - \frac{\epsilon_{sv}^r\epsilon_{vs}^r}{\epsilon_{ss}^r}) - N_n\Lambda_{vs} & \tau_\lambda & -N_n\frac{\epsilon_{ws}^r}{\epsilon_{ss}^r} \end{pmatrix}. \quad (3)$$

Here,  $\epsilon_{\alpha\beta}^r$  is dielectric tensor in coordinates given by Eq. (1),  $\tau_\lambda$  is the torsion of the ray, and  $\Lambda_{ij}$  is a tensor which contains information about the ray geometry (not shown here).

The eigensystem of the matrix  $\hat{T}$  consists of polarization vectors and wave numbers of the local characteristic waves: direct and reverse O and X modes with  $\pm N_t^O$  and  $\pm N_t^X$ , respectively. Following, for example, the Ref. [3], i.e. using the matrix of wave numbers  $\hat{D}$  and the diagonalization matrix (of eigenvectors)  $\hat{S}$ , Eq. (2) can be transformed to the form

$$\hat{D} = \hat{S}^{-1} \cdot \hat{T} \cdot \hat{S}, \quad \mathbf{F} = \hat{S}^{-1} \cdot \mathbf{f}, \quad \hat{\Gamma} = -\hat{S}^{-1} \cdot \frac{d\hat{S}}{ds}, \quad \frac{d\mathbf{F}}{ds} - i\frac{w}{c}\hat{D} \cdot \mathbf{F} = \hat{\Gamma} \cdot \mathbf{F}. \quad (4)$$

The left-hand side of the last equation describes the mode transfer due to both magnetic shear and plasma non-uniformity. Components of the vector  $\mathbf{F}$  are (complex) amplitudes of wave modes. The energy exchange between the two modes is proportional to the respective component of the coupling matrix  $\hat{\Gamma}$ . For the case of interest, the reverse waves with  $-N_t^{O,X}$  can be neglected.

The spurious mode, if generated, follows a trajectory different from the primary beam, causing splitting. The coupling between the primary and spurious wavemodes exists only within the common domain and stops when the beams are separated. Here, we apply a simple heuristic model to account for this effect. After performing ray-tracing for the reference ray, we perform pseudo-tracing with the same initial conditions but for another wave-mode. Since we are interested in investigating only the domain where the spurious ray is not far away from the reference ray, the plasma parameters for the pseudo-ray are assumed to be the same as for the primary one. The vicinity around each ray is weighted by Gaussian factor allowing us to estimate an overlap as  $e^{-d^2/(2b^2)}$ , where  $d(s)$  is the distance between the primary- and pseudo-rays, and  $b$  is the beam width. The non-overlapping part of the spurious ray is excluded from the wave-mode coupling.

**Implementation in TRAVIS code.** The model relies on ray tracing data, but the integration routine for Eq. (4) has to be separated from the ray tracing itself. The reason is that for solving Eq. (4) the co-moving coordinate system Eq. (1) is required, which can be constructed only after the reference-ray trajectory is known.

For numerical integration of Eq. (4), we separate the fast (related to  $\hat{D}$ ) from the slow (related to  $\hat{\Gamma}$ ) parts and integrate the equation with a fixed-step routine. The matrix  $\hat{T}$  is diagonalized numerically at every integration step. A correspondence of the eigensystem to the wave-modes is established by comparison of the eigenvalues and solutions of the local dispersion relations for O and X modes. Any case of degeneracy (non-distinguishable values of  $N_i^O$  and  $N_i^X$  or the cutoff for one of the modes) needs to be considered separately.

The matrix  $\hat{S}$  can be constructed when the eigenvectors of  $\hat{T}$  are found. These eigenvectors are not unique in a sense that they can be multiplied by arbitrary functions of  $s$ , as can be seen from the first Eq. (4). In our case, however,  $\hat{\Gamma}$  is a function of  $d\hat{S}/ds$ . This ambiguity is essential for the coupling equations but can only affect the results within the accuracy of the model. We thus normalize the eigenvalues to unity and calibrate them in such a way that they vary smoothly. In order to test the validity of the numerical algorithm, the results have been benchmarked against simple test-cases that use analytical calibrations [2].

In order to minimize the polarization mismatch for the RF beam and to guarantee the highest wave-mode purity in the plasma, we have implemented several auxiliary TRAVIS modules. These include a polarization calculation at plasma/vacuum boundaries, the evolution of the mode purity in plasma, and estimation of the beam splitting. For O2 multi-pass scenarios, a drop of the mode purity due to the difference of magnetic field vector at the exit and re-entrance points is taken into account as well as possible scrambling on the mirrors.

**Results.** We have applied the developed tools for verification of several W7-X scenarios. The first example, an oblique ( $20^\circ$ ) launch of the X2 mode in plasma of  $n_e \approx 10^{20} \text{ m}^{-3}$ , was considered with various density profiles; magnetic shear was small. In Figure 1, the role of gradient sharpness and location of the resulting wave-mode energy exchange is shown. In agreement with our expectations a higher density gradient results in a higher mode conversion ratio.

Figure 2(left) illustrates the roles of the "split" and "in-ray" components of the spurious mode. We see a gradual increase of the split part that saturates eventually after passing through the high-gradient zone. The in-ray part continues the energy exchange with the primary mode in the form of modulations. In Figure 2(right) we see a promising effect of an improvement of an initially low beam purity. Under certain initial conditions the "O to X" energy conversion may appear even if the X mode is dominating. The exact criteria for this are to be clarified. However, the effect does not appear if the initial amplitude of the spurious mode is very small.

Modeling of the multipass O2 scenario indicates possible depolarization during the second entrance, with the energy loss up to 15%. Depolarization is not symmetric, so the beam profile is no longer Gaussian during the second pass.

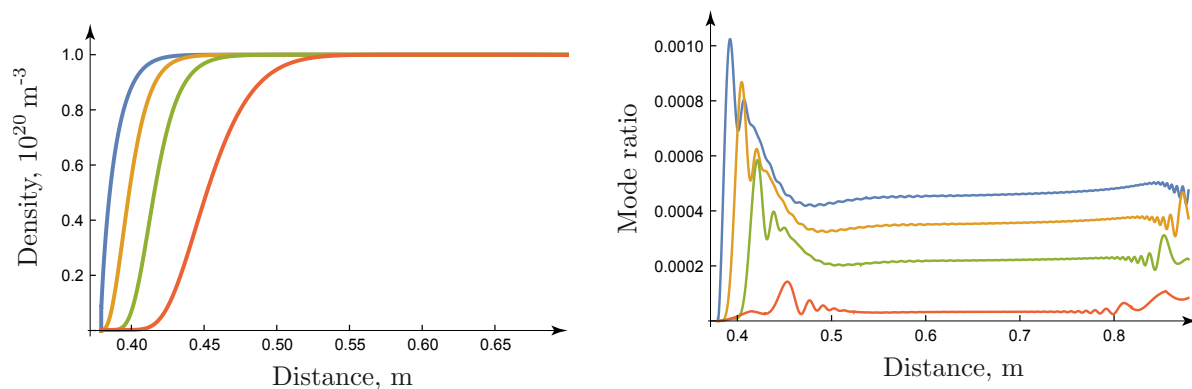


Figure 1: X2-O2 coupling along the ray (small shear). Left:  $n_e(s)$  with different gradients; Right: Spurious O2 mode rate evolution; colors the same as in (left).

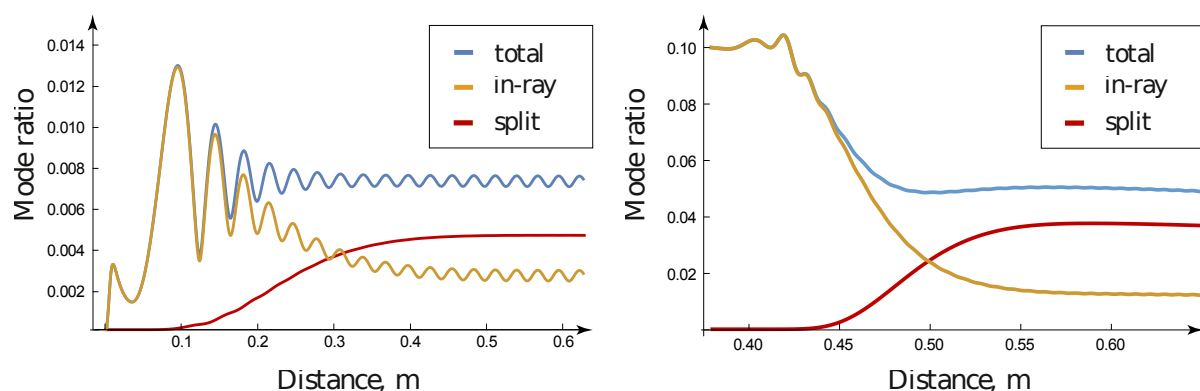


Figure 2: Examples of mode coupling in W7-X for different modes with different initial purities.

Currently, we are performing a benchmarking against a full-wave calculations. We have achieved a qualitative agreement, however the full-wave results tend to exhibit several times higher mode conversion rates. Whether this is due to the overly-simplified model or disharmonious initial conditions is not clear yet.

**Summary.** We have developed tools to investigate and optimize ECRH efficiency. In the low-shear W7-X device, the impact of mode transition is very limited and can be neglected in the zeroth approximation. Nevertheless in scenarios with very high density gradient, adjusting the initial conditions can be helpful. For secondary entrances of beams reflected by walls or mirrors significant depolarization occurs. This could potentially be fixed by installing polarizers on the walls at the targeted places of reflection.

## References

- [1] K. Nagasaki et al, Phys. Plasmas **6**, 556 (1999)
- [2] R. Dumont, G. Giruzzi, Phys. Plasmas **6**, 660 (1999)
- [3] S. E. Segre, V. Zanza, Phys. Plasmas **18**, 092107 (2011)
- [4] N.B. Marushchenko, Y. Turkin, H. Maassberg, Comp. Phys. Comm. **185**, 165-176 (2014)